Research paper

'Temporary Plasticiser': A novel solution to fabricate 3D printed patient-centred cardiovascular 'Polypill' architectures

Beatriz C. Pereira[a], Abdullah Isreb[a], Robert T. Forbes[a], Filipa Dores[a], Rober Habashy[a], Jean-Baptiste Petit[a], Mohamed A. Alhnan[b,*], Enoche F. Oga[a,*]

[a] School of Pharmacy and Biomedical Sciences, University of Central Lancashire, Preston, Lancashire, UK
[b] Institute of Pharmaceutical Sciences, King's College London, London, UK

ARTICLE INFO

ABSTRACT

Hypertension and dyslipidaemia are modifiable risk factors associated with cardiovascular diseases (CVDs) and often require a complex therapeutic regimen. The administration of several medicines is commonly associated with poor levels of adherence among patients, to which World Health Organisation (WHO) proposed a fixed-dose combination unit (polypill) as a strategy to improve adherence. In this work, we demonstrate the fabrication of patient-specific polypills for the treatment of CVDs by fused deposition modelling (FDM) 3D printing and introduce a novel solution to meet critical quality attributes. The construction of poly(vinyl alcohol) (PVA)-based polypills containing four model drugs (lisinopril dihydrate, indapamide, rosuvastatin calcium and amlodipine besylate) was revealed for the first time. The impact of tablet architecture was explored using multi-layered and unimatrix structures. The novel approach of using distilled water as a 'temporary co-plasticiser' is reported and was found to significantly lower the extruding (90 °C) and 3D printing (150 °C) temperatures from 170 °C and 210 °C respectively, with consequent reduction in thermal stress to the chemicals. XRD indicated that lisinopril dihydrate and amlodipine besylate maintained their crystalline form while indapamide and rosuvastatin calcium were essentially in amorphous form in the PVA tablets. From the multilayer polypills, the release profile of each drug was dependent on its position in the multilayer. In addition to the multilayer architecture offering a higher flexibility in dose titration and a more adaptive solution to meet the expectations of patient-centred therapy, we identify that it also allows orchestrating the release of drugs of different physicochemical characteristics. Adopting such an approach opens up a pathway towards low-cost multidrug delivery systems such as tablets, stents or implants for wider range of globally approved actives.

1. Introduction

Despite advances in the treatment of cardiovascular diseases (CVDs), they are still the leading cause of morbidity and mortality worldwide [1]. For CVDs, the impact of non-adherence has been associated with an increased risk in all-cause mortality, recurrent myocardial infarction, stroke or transient ischaemic attacks [2–4]. Adherence to therapy decreases with increasing number of medicines taken. For instance, only 40% of individuals hospitalised for acute coronary disease achieve adherence [5,6]. However, treatment with a polypill increased adherence by 44% compared with usual treatment, in patients with CVD or at high risk of CVD [7].

The concept of fixed multidrug combinations (polypills) was initially proposed in 2001 by the WHO and The Wellcome Trust as an intervention for non-communicable diseases [8]. Wald and Law (2003) proposed the polypill as a preventive strategy to reduce CVDs by more than 80%. A daily treatment with a six-component polypill (antiplatelet, beta-blocker, angiotensin converting enzyme (ACE) inhibitor, diuretic, statin and folic acid) would have a preventive effect in cardiovascular disease in individuals over 55 years or with known occlusive vascular disease, by decreasing CV risk factors [9]. A step further was taken when the first multicomponent formulation (Furder-CNIC-Ferrer polypill) was approved and commercialised, under the brand names Trinomia®, Sincronium® and Iltria® by Ferrer Pharmaceuticals [10].

The manufacture of a polypill poses a number of significant technical, formulation, processing and stability challenges as well as clinical considerations. It is well-known that combining multiple active pharmaceutical ingredients (APIs) will increase the potential of adverse effects [11]. Therefore, the composition of the dose combination should ideally be individualised to provide a 'best-fit' solution for each patient

---

to meet changing treatment targets, the patient's response and preferences and unwanted adverse effects. In addition, the inclusion of multiple molecules with different chemical and physical characteristics can precipitate both drug-drug and drug-excipient interactions, with significant implication on long term dose stability. Combinations of drugs with significantly different doses is also an analytical and formulation challenge.

The concept of a polypill has been highly criticised for delivering a 'generic solution' that does not accommodate changing patients' needs and preferences [12]. In addition, the use of traditional large manufacturing facilities to produce an individualised patient dose is likely to be too expensive and an impractical option [13]. Employing 3D printing provides a potential alternative with its low cost, malleability to network commands and digital programming, minimal space/ logistic requirements as well as its highly adaptive nature. Previous attempts towards individualising 'polypill' tablets have been achieved *via* extrusion-based 3D printing, where multiple drugs have been incorporated to achieve immediate and extended drug release for 3 or 5 model drugs [14,15]. However, this approach requires a post-printing drying process and often resulted in tablets with fragile and deformed structure upon solvent evaporation [14]. Fused deposition modelling (FDM) 3D printing has therefore been proposed as an alternative method for 3D printing of tablets [16,17] and medical devices [18]. The method allows the fabrication of immediate [19–21], delayed [22,23], extended release tablets [24–28] as well as for dual drug delivery systems [29–31]. The technology offers several advantages such as the lower cost, absence of finishing step, small place requirement and obviation for material recycling [13,32]. Despite these merits, FDM 3D printing has been associated with a loss in drug contents due to thermal degradation during hot melt extrusion (HME) and FDM 3D printing [13,19,24,32]. Therefore, it is of particular importance to mitigate the risk of drug degradation by lowering both extrusion and printing temperature.

Poly (vinyl alcohol) (PVA) has proven to be suitable in the fabrication of controlled-release tablets by 3D printing tablets by FDM 3D printing [16,17,24,33–37]. Initially drug loading was achieved by incubation of the filament in saturated organic solutions with printing temperature of 250 °C [17]. Incorporation of the drug by hot melt extrusion has been performed at 180 °C and printing at 195 °C [35]. Such high temperatures can compromise the integrity of drugs with lower degradation temperatures. The earlier study also yielded tablets with extended release behaviour rather than a rapid release [35].

In this work, a polypill was designed and fabricated by FDM 3D printing to provide an individualised, multi-drug solution for the treatment of cardiovascular patients. Several potential critical quality attributes have been explored. The impact of polypill structure (multilayer versus unimatrix) and the order of these layers within the multilayer structure on the release profile has been investigated. Multilayer tablets are an established method for combined oral administration of drugs [38,39]. Four model drugs were employed in this study following National Institute for Health and Care Excellence (NICE) and Joint National Committee (JNC) guidelines for the prevention and treatment of CVDs [40,41]. The use of different matrices for each drug allows the separation of the active components physically, avoiding

incompatibilities and flexibility in the tailoring of each dose. A multilayer tablet also has the potential of modifying the release profile of each drug, with changes of each matrix and the sequential order of the polypill. We also report a novel solution to enable lower temperature extrusion and FDM 3D printing by adopting a novel 'temporary plasticiser' approach with a newly developed immediate release grade PVA.

2. Materials and methods

2.1. Materials

Lisinopril dihydrate, indapamide, amlodipine besylate and rosuvastatin calcium were purchased from Kemprotec Ltd (Cumbria, UK). Titanium dioxide was obtained from Sigma-Aldrich, Inc. (Gillingham, UK). HPLC gradient grade acetonitrile and methanol were from Fisher Scientific Ltd (Loughborough, UK). Sorbitol and poly(vinyl alcohol) (Parteck MXP) were donated by Merck (Darmstadt, Germany). Parteck MXP is a polymer developed for hot melt extrusion which is also Generally Recognised as Safe (GRAS) by the US Food and Drug Administration and compliant with the US, European and Japanese pharmacopeias for excipients monographs [42]. All other materials were of analytical grade and commercially available.

### 2.2. Preparation of the filaments using hot melt extrusion (HME)

Filaments containing individual drugs at different concentrations were manufactured to deliver the individual target dose of each model drug (Table 1). In an attempt to decrease the extrusion and printing temperatures, water was used as a temporary co-plasticiser along with sorbitol. Titanium dioxide (TiO$_2$) was added to the formulation of all individual drug filaments except amlodipine besylate, as it catalysed its chemical degradation (data not shown). A Thermo Scientific HAAKE MiniCTW hot melt extruder (Karlsruhe, Germany) with standard counter flow conical twin-screws of two stages conveying domains (22 cm) was used to prepare the filaments. Blank (drug-free), individual drug loaded and multidrug (for unimatrix tablet) filaments were prepared by blending 10 g of dry ingredients with additional 2 g of distilled water (temporary plasticiser) (Table 1) using mortar and pestle and then fed to the hot melt extruder at 90 °C and mixed at 100 rpm for 5 min. The filaments were extruded at the same temperature at 35 rpm. The extruded filaments were dried at 100 °C at 0% RH for 1 hr in a FD240 Binder heating chamber (Tuttlingen, Germany). For comparison purposes, a blank and drug loaded filaments were also processed via HME without water at 170 °C and extruded as described above.

2.3. Tablet design and 3D printing

The tablets printed were designed using Autodesk® 3ds Max Design 2016 software version 18.0 (Autodesk, Inc., USA). The designs were then imported to the computer software in stereolithographic (STL) format. The extruded filaments were printed by a Makerbot 2x 3D printer (Makerbot Industries, NY, USA) fitted with 0.4 mm nozzle and controlled by Simplify 3D software version 4.0 (Cincinnati, OH, USA). Printing took place using

Table 1
Ingredients of HME based filament containing a single drug (for multilayer tablets) or multiple drugs (for unimatrix tablet).

Filament	Ingredients							Nozzle size (mm)
	Lisinopril dihydrate	Amlodipine besylate	Indapamide	Rosuvastatin calcium	PVA	Sorbitol	TiO$_2$	
Blank filament (drug free)					70%	30%		1.7
Lisinopril dihydrate filament	20%	–	–	–	56%	23%	1%	1.5
Amlodipine besylate filament	–	10%	–	–	63%	27%	–	1.5
Indapamide filament	–	–	5%	–	66.5%	27.5%	1%	1.7
Rosuvastatin calcium filament	–	–	–	20%	56%	23%	1%	1.7
Unimatrix filament	5%	2.5%	1.25%	5%	60.35%	25.9%	–	1.7
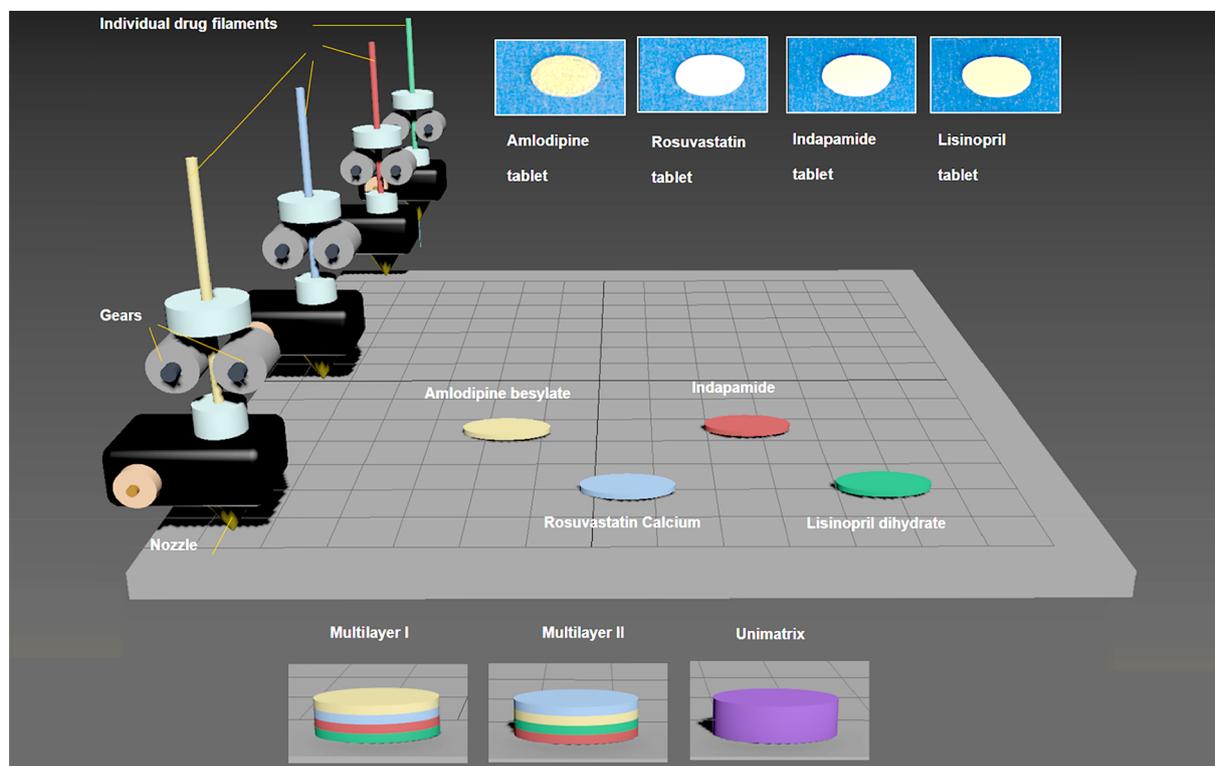
Fig. 1. 3D schematic diagram of FDM 3D fabrication of PVA-based polypills containing four drugs. (A) Filaments loaded with individual model drugs (lisinopril dihydrate, amlodipine besylate, indapamide and rosuvastatin calcium) were fabricated using HME used as feed to fabricate individual tablets (B) or used to fabricate 3D printed tablet with multilayer structure (polypill I and polypill II). (C) Rendered images and photographs of 3D printed polypill based 3D with multilayer structure of Polypill I: lisinopril, indapamide, rosuvastatin and amlodipine (top to bottom) and Polypill II: rosuvastatin, amlodipine, lisinopril and indapamide (top to bottom). For ease of comparison, polypill tablet of unimatrix structure with same dimensions and drug doses were fabricated from a single filament.

nozzle and building plate temperatures of 150 and 40 °C respectively. The tablets were printed following a concentric fill pattern and 100% infill with a layer thickness of 166 µm. Blank, individual drug and polypill (Unimatrix) were printed with the corresponding filaments. Polypills (Multilayer I and II) (Fig. 1) were printed in two steps: the two nozzles of the 3D printer were initially used to print the first two layers, followed by thorough cleaning before printing the third and fourth layers. Different drug layers were printed using identical x-y position with 0.5 mm increase in z-axis for each additional layer. Tablets were fabricated by sequential printing of a sequence of ten tablets. For comparison reasons, blank tablets (without the addition of water) were printed using the same settings as above but at a nozzle temperature of 210 °C.

2.4. Thermal analysis

Samples of the raw materials, drug-loaded filaments and 3D printed tablets were analysed by differential scanning calorimetry (DSC) and thermogravimetric analysis (TGA). A TGA Q500 (TA Instruments, Elstree, Hertfordshire, UK) was used to characterise about 10 mg of each material. Samples were heated at a rate of 10 °C/min from 25 to 500 °C with a nitrogen purge of 40:60 mL/min for sample: furnace respectively. In addition, a DSC Q2000 (TA Instruments, Elstree, UK) was used to assess the thermal behaviour of the aforementioned samples. Each sample (5 mg) was scanned from −50 to 200 °C at 10 °C/min using a nitrogen purge of 50 mL/min. TA Universal analysis software (v 4.5A, TA Instruments, Elstree, UK) was used to evaluate the data after collection in both TGA and DSC.

DSC was also used to study the effect of water content on the glass transition temperature (Tg) of the polymer in the extruded filaments at three different time points: on freshly extruded filaments, on filaments dried for 1hr and on filaments dried for 4 hrs (Section 2.2). All measurements were done in triplicates.

2.5. X-ray diffractometry (XRD)

XRD analysis was performed on raw materials, blank filaments, drug-loaded filaments and 3D printed tablets in order to assess the crystalline structure of the model drugs. Samples were measured using a silica low-background sample holder and an X-ray diffractometer, D2 Phaser with Lynxeye (Bruker, Germany). Samples were scanned between 2Theta = 5° to 50° using a 0.01° step width and a 1.25 sec time count. The divergence slit was 1 mm and the scatter slit 0.6 mm. The wavelength of the X-ray was 0.154 nm using a Cu source and a voltage of 30 kV. Filament emission was 10 mA using a scan type coupled with a theta/theta scintillation counter over 60 min.

2.6. Drug content analysis via high performance liquid chromatography (HPLC)

An HPLC method for simultaneous quantification of the four model drugs was developed, validated, and utilised in drug content analysis and dissolution testing (Fig. S1). HPLC analysis was performed using Agilent 1260 series UV-HPLC (Agilent Technologies, Germany) equipped with a Synergi Max column (250 × 4.6 mm, 4 µm particle size) (Phenomenex, Macclesfield, UK) at temperature 20 °C. Analysis was carried out at a detection wavelength of 210 nm, a flow rate of 1 mL/min, an injection volume of 100 µL and a 35 min run time. The mobile phase consisted of a gradient of solvent A (acetonitrile) and solvent B (water adjusted to pH 3 with phosphoric acid). Each run started at a composition of 17:83 from 0 till 4 min, followed by a gradient of 17:83 to 20:80 from 4 to 6 min, and then by a gradient of 20:80 to 90:10 from 6 to 32 min. Between 32.01 and 35 min, the gradient was increased to 17:83. The retention time for lisinopril dihydrate, amlodipine besylate, indapamide and rosuvastatin calcium was 3.6, 14.5, 20.5, and 21.4 min respectively. The limit of detection was 0.52, 0.18,

0.55 and 0.79 mg/L, with a limit of quantification of 1.57, 0.54, 1.67 and 2.41 mg/L for lisinopril dihydrate, amlodipine besylate, indapamide and rosuvastatin calcium respectively.

Drug content in the filament and tablets was assessed by accurately weighing each sample and dissolving it in a 1000 mL of a water: acetonitrile: methanol (80:10:10) mixture. The solutions were then filtered through an Econofltr 0.22 µm syringe (Agilent Technologies, Cheadle, UK) and analysed by HPLC. Drug contents of polypill (Multilayer I and II) were calculated based on the assumption that each drug layer corresponds to an equivalent proportion of the tablet.

2.7. Scanning electronic microscopy (SEM)

The morphology and cross-section of the Multilayer I and II and Unimatrix polypills were assessed using a JCM-6000 plus NeoScope™ microscope (Jeol, Tokyo, Japan) at 10 kV. All samples were gold coated using a JFC-1200 Fine Coater (Jeol, Tokyo, Japan). The images were collected using Image J software version 1.2.0. (Tokyo, Japan).

2.8. Dissolution studies

The *in vitro* release profile of 3D printed individual drug tablets and polypills was assessed using a USPII dissolution test apparatus Erweka DT600HH dissolution tester (Heusenstamm, Germany) with a paddle rotation speed of 50 rpm in 900 mL of 0.1 M HCl (pH 1.2) at 37 ± 0.5 °C. Due to amlodipine sensitivity to metal and light, the dissolution test of amlodipine besylate and the polypills was carried out in a dark room and paddles of the dissolution bath were carefully sealed with PTFE coated glass cloth adhesive tape (Viking Industrial Products, Keighley, UK) to avoid possible

interaction of the drug with the stainless steel [43]. The experiments were performed in triplicate for each tablet. Aliquots were manually collected (5 mL) using an Econofltr 0.2 µm syringe filter (Agilent Technologies Ltd., Cheadle, UK) at time points: 5, 10, 15, 20, 30, 45, 60, 90 and 120 min. The samples were analysed by the HPLC method as described in Section 2.6.

2.9. Statistical analysis

Statistical analysis of the results were done using paired *t*-test on the SPSS software (22.0.0.2). Differences in the results below the probability level of $p < 0.05$ were considered significant.

3. Results and discussion

A polymeric matrix platform for the delivery of four model drugs based on PVA as a carrier matrix polymer has been developed. An oval-shaped design was used to produce printed tablets loaded with a single drug (height = 0.5 mm) (Fig. 1a and b). Later, a polypill tablet of multilayer architecture was designed and fabricated by the superimposition of four layers of the model drugs using the previous design with two different layer orders (Multilayer I and II) and a total tablet height of 2.0 mm (Fig. 1c). The design was adapted with the same x-y section across z-axis to maintain identical dimension foreach drug layer. The polypill was also constructed following a unimatrix architecture containing the four model drugs in one monolithic structure with identical oval geometry and dimensions.

Thermal analysis was performed in order to assess the stability of the four model drugs under the processing temperatures of HME and FDM 3D printing (Fig. 2). PVA showed a 2% decrease of weight loss due
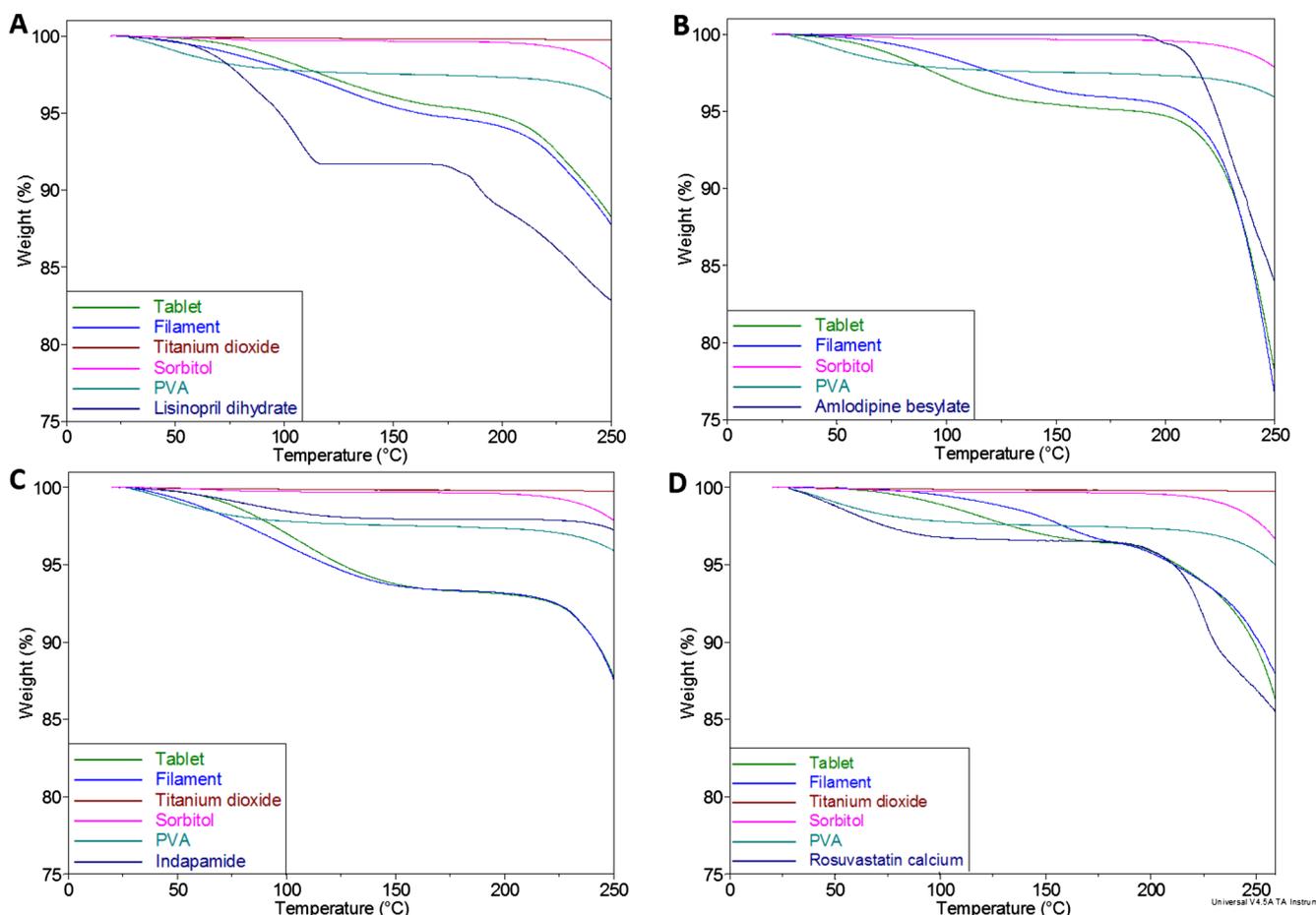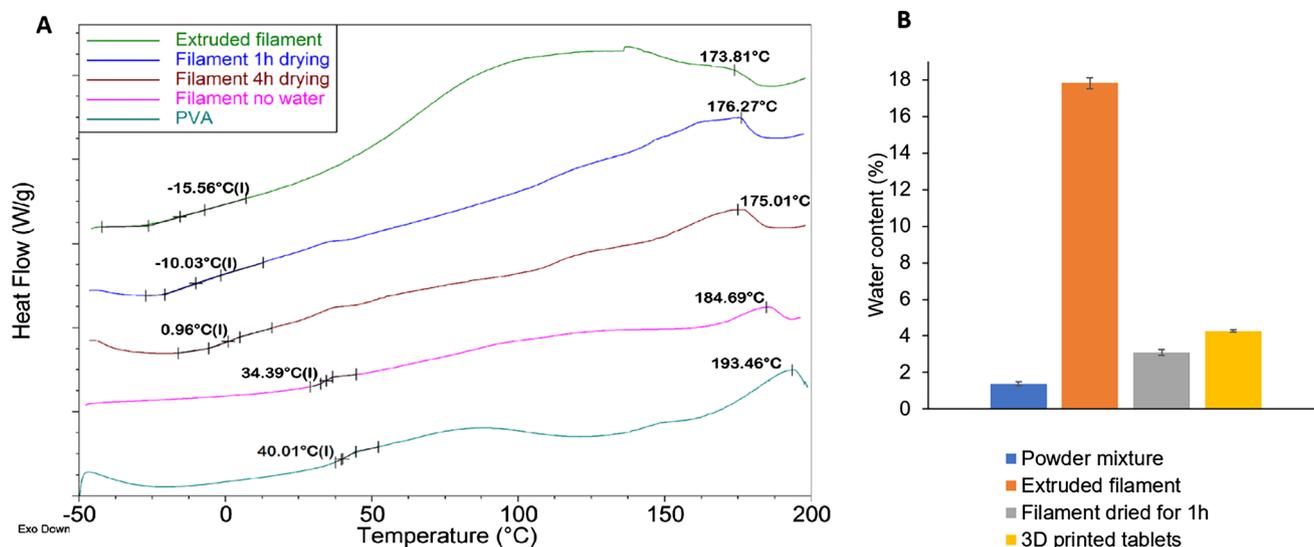

Fig. 2. TGA thermal degradation profiles of raw APIs, PVA, sorbitol, titanium dioxide and API-loaded filaments and 3D printed tablets for (A) lisinopril dihydrate, (B) amlodipine besylate, (C) indapamide and (D) rosuvastatin calcium.

Fig. 3. (A) DSC thermograph of extruded filament, 3D printable filament (dried for 1 hr at 105 °C) and filament dried until stable weight obtained. (B) Water content for drug-free powder blend (control), powder with water for extrusion, extruded filament, 3D printable filament (dried for 1 hr at 105 °C), and 3D printed tablet.

Table 2
Drug contents in filament with and without temporary co-plasticiser (n = 3).

Drug	Drug contents in individual filaments ± SD (%)		Drug content in unimatrix filaments ± SD (%)	
	Plasticised with sorbitol (without water, 170 °C)	Plasticised with water and sorbitol (90 °C)	Plasticised with sorbitol (without water, 170 °C)	Plasticised with water and sorbitol (90 °C)
Lisinopril dihydrate	3.3 ± 0.43	93.9 ± 1.66	20 ± 4.70	99.2 ± 2.9
Amlodipine besylate	75.5 ± 0.39	97.89 ± 1.94	7.3 ± 3.70	92.8 ± 8.1
Indapamide	84.4 ± 1.26	93.32 ± 1.67	100.3 ± 0.14	95.4 ± 5.2
Rosuvastatin calcium	88.0 ± 1.26	98.2 ± 1.09	37.2 ± 6.93	92.1 ± 2.8

to presumed water evaporation followed by a degradation at temperature > 250 °C (Fig. 2a) [42]. The thermal decomposition profile of the four drugs used on this experiment revealed a weight loss at 130 °C of 0% for amlodipine and about 8%, 2% and 3.3% for lisinopril, indapamide and rosuvastatin respectively. The weight losses can be attributed to the moisture content of each drug [44,45] (Fig. 2a). All drugs exhibited a thermal degradation > 200 °C while rosuvastatin revealed a second phase of degradation at around 230 °C. Therefore, based on the thermal profiling above, it was necessary to target lower processing temperatures to avoid drug degradation.

Consideration of the DSC thermograph indicated that PVA showed a glass transition temperature (Tg) at 45 °C and an endotherm peak at 192 °C (Fig. 3a), which is consistent with previous findings and can be explained by the melting of the crystals within the semi-crystalline nature of this polymer [46]. It is therefore essential to employ an HME temperature > 180 °C to ensure the complete melting of the crystalline domain in PVA structure and allow the smooth extrusion of the polymer filament. One established approach to lower the processing temperature of HME is through the use of a plasticiser [47]. In fact, sorbitol has been previously used to plasticise PVA to achieve an extruding temperature of 140 °C [48,49]. It has been proposed that hydroxy groups in sorbitol molecule can form hydrogen bonds with PVA and hence weaken PVA interchain interactions leading to a reduced glass transition temperature (Tg) and facilitated thermal processing [50]. However, the use of such a high concentration of plasticiser would yield a highly flexible filament that is incompatible with FDM 3D printing process. On the other hand, an extruded filament of PVA/sorbitol (70:30) composition (providing a Tg of 55 °C) is compatible for FDM 3D printing. However, preliminary studies identified that it requires a high temperature for extrusion and FDM 3D printing (180 and 220 °C respectively), which

will result in the degradation of the model drugs (Table 2).

In this paper, we investigate a novel approach of utilising an evaporable plasticiser, that can initially facilitate polymer extrusion, and then followed by its partial or complete removal (in a secondary step) is able to restore filament mechanical rigidity towards printer ready robustness. Water was proposed as a solvent due to its proven plasticising properties (Tg of −135 °C [51]), its safety profile, its low cost and its ability to evaporate. The addition of water (at a weight equivalent of 20% of the blend) enabled the extrusion of PVA/sorbitol filament (drug free) at a significantly decreased temperature of 90 °C. The drop in the Tg of the filament to approximately −15 °C results in a highly flexible filament, that proved to be incompatible to FDM 3D printer's nozzle (Fig. 3a). However, when the resultant filaments were dried for 1 hr at 100 °C, the drying process reduced the water content in the filament by 14.15 ± 0.07% (out of the 16.67% added) and reduced the flexibility of the filament (with a Tg value of −10 °C). The resultant filaments were deemed appropriate for FDM 3D printing at a temperature of 150 °C and on printing yielded 3D printed tablets that showed a water loss of 4.28 ± 0.05% (Fig. 3b). After this successful outcome, the approach was employed to compound filaments now loaded with individual model drugs or their blends (for Unimatrix polypill). Water has proven to be a suitable plasticiser for cellulose, polyvinylpyrrolidone and polyvinyl acetate based polymers [52]. Hence, this reported approach might be applicable to these polymers. However, other polymers, particularly water sensitive species such as poly(anhydrides) [53], may suffer hydrolytic degradation and are likely to be incompatible with this developed method.

Filaments of individual drugs showed a mean content of 93.9 ± 1.7%, 97.9 ± 1.9%, 93.3 ± 1.7% and 98.2 ± 1.1% for lisinopril dihydrate, amlodipine besylate, indapamide and rosuvastatin
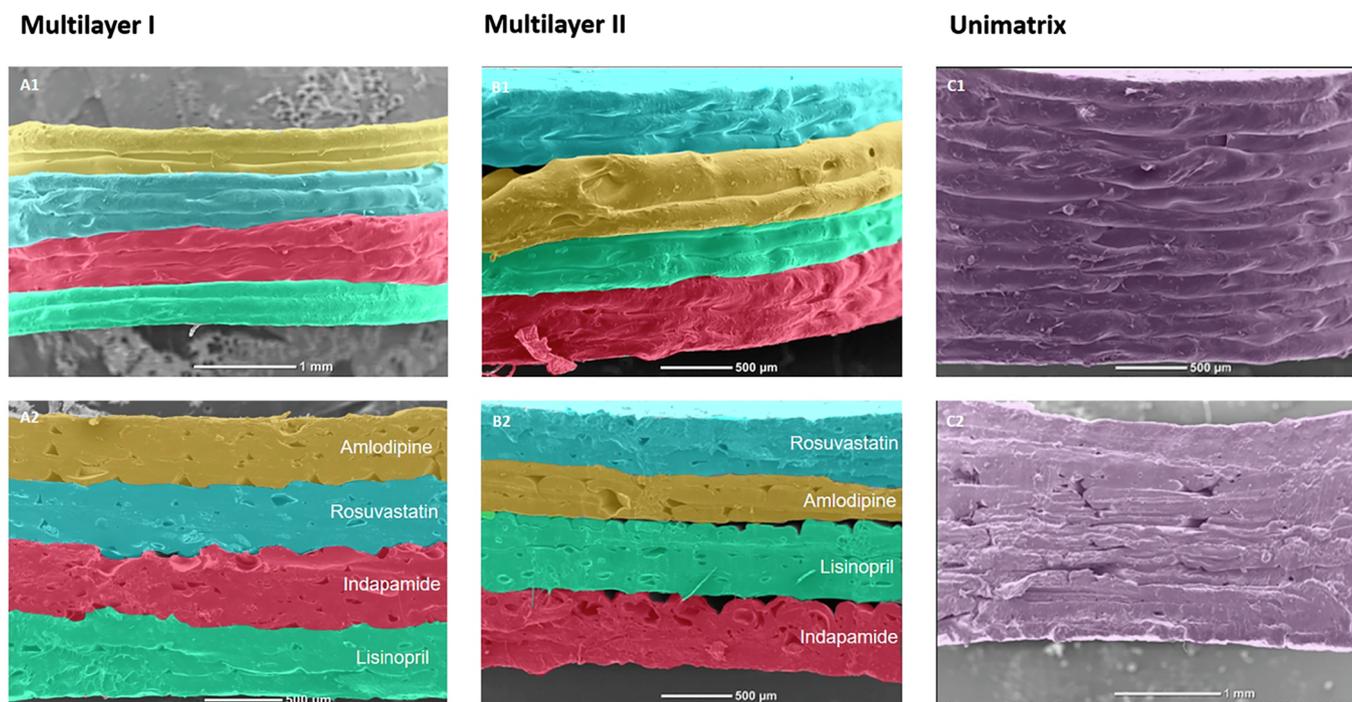
Multilayer I

Multilayer II

Unimatrix

Fig. 4. False-coloured SEM images of the surface and cross-section of (A1 and A2) polypill I, (B1 and B2) polypill II and (C1 and C2) unimatrix respectively. Each individual drug layer is highlighted with a distinctive colour; lisinopril (yellow), amlodipine (orange), indapamide (green) and rosuvastatin (blue).

calcium, respectively (Table 2). The use of a higher processing temperature had a negative effect on the integrity of the model drugs particularly for lisinopril (3.4%) (Table 2). The drug content obtained was only possible to achieve through the significant decrease in the processing temperature (90 °C) permitted with the addition of water as a temporary co-plasticiser.

The inclusion of the four drugs in the one filament (for production of the Unimatrix polypill) resulted in a similar range of values for drug content. This finding suggested minimal chemical interaction between the four drug ingredients during their processing together at 90 °C.

Turning now to consider how much drug is lost in the conversion of the filament into a tablet; individual drug loaded filaments printed into tablets for indapamide and rosuvastatin calcium gave tablet drug content recoveries of 96.1 ± 2.1% and 95.4 ± 2.4%, respectively (Table 2). However, amlodipine besylate and lisinopril dihydrate tablets produced from their filaments showed lower recoveries of 90.7 ± 2.2 and 87.5 ± 1.5% respectively.

Two polypills (Multilayer I and II) with different layer sequences have been designed and 3D printed. Multilayer I was 3D printed with the external layers of the most soluble drugs in aqueous medium [amlodipine besylate (380 mg/L) and lisinopril dihydrate (97,000 mg/L)] while the internal layers comprised the two least soluble drugs [indapamide 9.5 mg/L and rosuvastatin calcium (~18 mg/L)] [54,55].

Multilayer II structure contained the two least soluble drugs as external layers and the most soluble as internal layers. SEM images of the surface of Multilayer I and II designs showed the individual sections of each drug (Fig. 4a1, b1). Each compartment consisted of three 166 μm-layers, which were also visible in the cross-section of the tablets (Fig. 4a2, b2). The unimatrix polypill was printed in a continuous process and showed more uniform layers on its surface (Fig. 4c1, c2).

The dimensions, weight and drug content of the 3D printed tablets were determined (Tables 2 and 3). The weight of the polypill tablets (whether multilayer or unimatrix format) corresponded to the sum of the four individual layers. The drug content of each drug in both Multilayer I and II was expected to be similar to the individual tablets, since the layers are fabricated using the same filaments. The results in Table 3 reveal variations in the expected drug contents for the multilayer structure that can be explained by deviations in the weight of each layer produced during printing process. This could not be accounted for by the calculation method, which assumes an equal weight distribution between the four model drug layers.

DSC scans obtained for both filaments and tablets of containing a single drug consistently showed a glass transition temperature event at around −10 °C following an initial first heating ramp. The value is in line with that observed with the blank filaments. However, the Tg values indicated from DSC scans after a second heating run were markedly

Table 3
Dimensions, weight uniformity and drug contents in filament and corresponding 3D printed polypills (unimatrix or multilayer) n = 3.

Tablet	Dimension ± SD (mm)			Weight Uniformity ± SD (mg)	Drug contents in tablets ± SD (%)			
	X	Y	Z		Lisinopril	Amlodipine	Indapamide	Rosuvastatin
Lisinopril dihydrate	12.88 ± 0.12	7.98 ± 0.08	0.59 ± 0.07	49.4 ± 5.6	87.8 ± 1.5			
Amlodipine besylate	12.89 ± 0.09	7.89 ± 0.1	0.62 ± 0.03	51.58 ± 1.6		90.68 ± 2.28		
Indapamide	12.99 ± 0.18	7.92 ± 0.15	0.55 ± 0.69	51 ± 3.2			96.06 ± 2.06	
Rosuvastatin calcium	13.12 ± 0.08	8.1 ± 0.09	0.53 ± 0.04	51.2 ± 0.75				95.4 ± 2.37
Unimatrix	12.9 ± 0.07	8.17 ± 0.08	1.95 ± 0.05	199.03 ± 6.81	100.6 ± 2.8	87.5 ± 0.3	96.3 ± 1.9	88.9 ± 3.9
Multilayer I[*]	12.8 ± 0.14	8.03 ± 0.11	1.93 ± 0.07	179.88 ± 6.51	82.9 ± 2	101.8 ± 1.7	92.4 ± 4.6	99.9 ± 1.0
Multilayer II[*]	12.89 ± 0.15	7.96 ± 0.11	1.83 ± 0.15	197.92 ± 5.4	90.3 ± 2	95.7 ± 3.9	88.7 ± 3.8	101.5 ± 2.4

* Multilayer I and II were produced using individual drug loaded filaments detailed in Table 2.
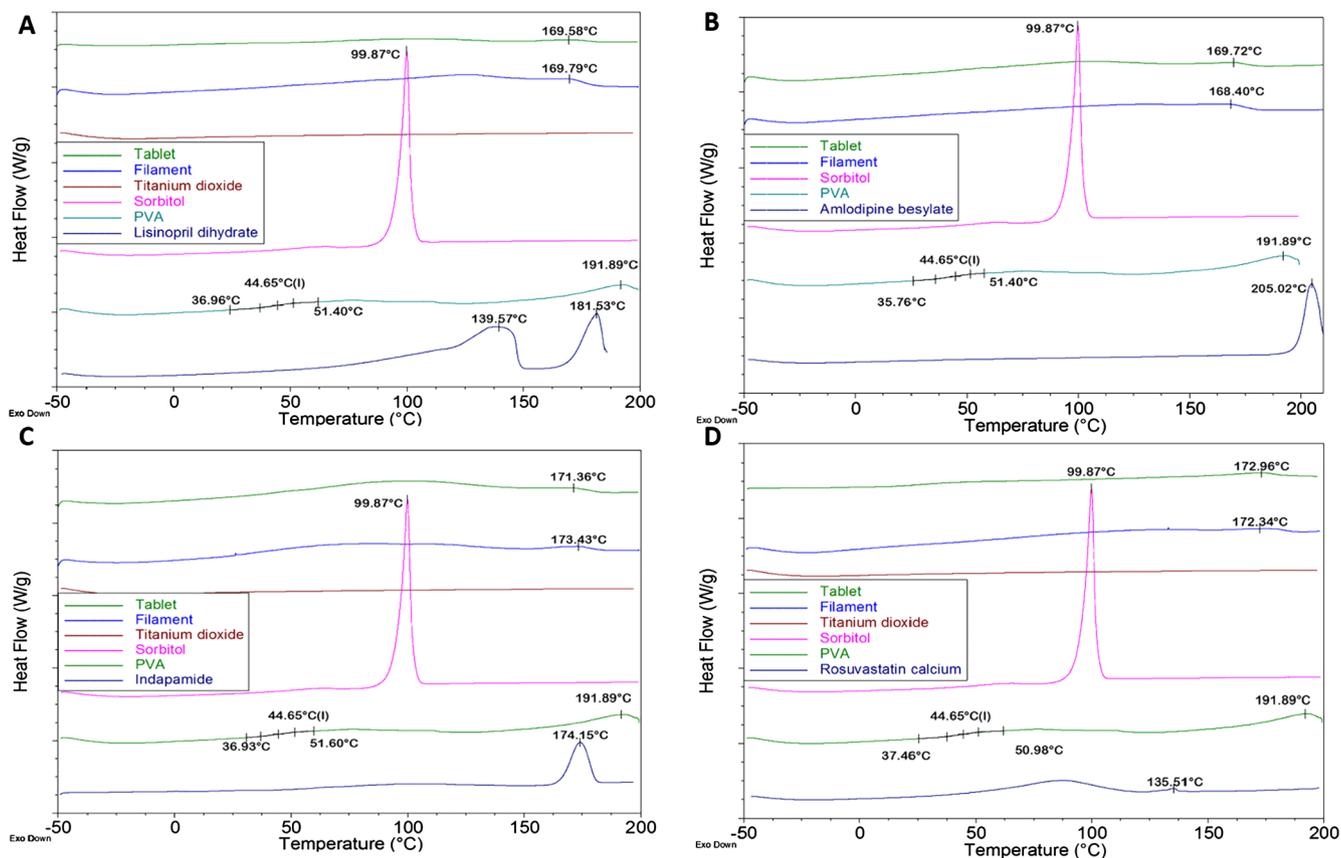
Fig. 5. DSC thermographs (first run) of raw APIs, PVA, sorbitol, titanium dioxide, blank filament and API-loaded filaments and 3D printed tablets for (A) lisinopril dihydrate, (B) amlodipine besylate, (C) indapamide and (D) rosuvastatin calcium.
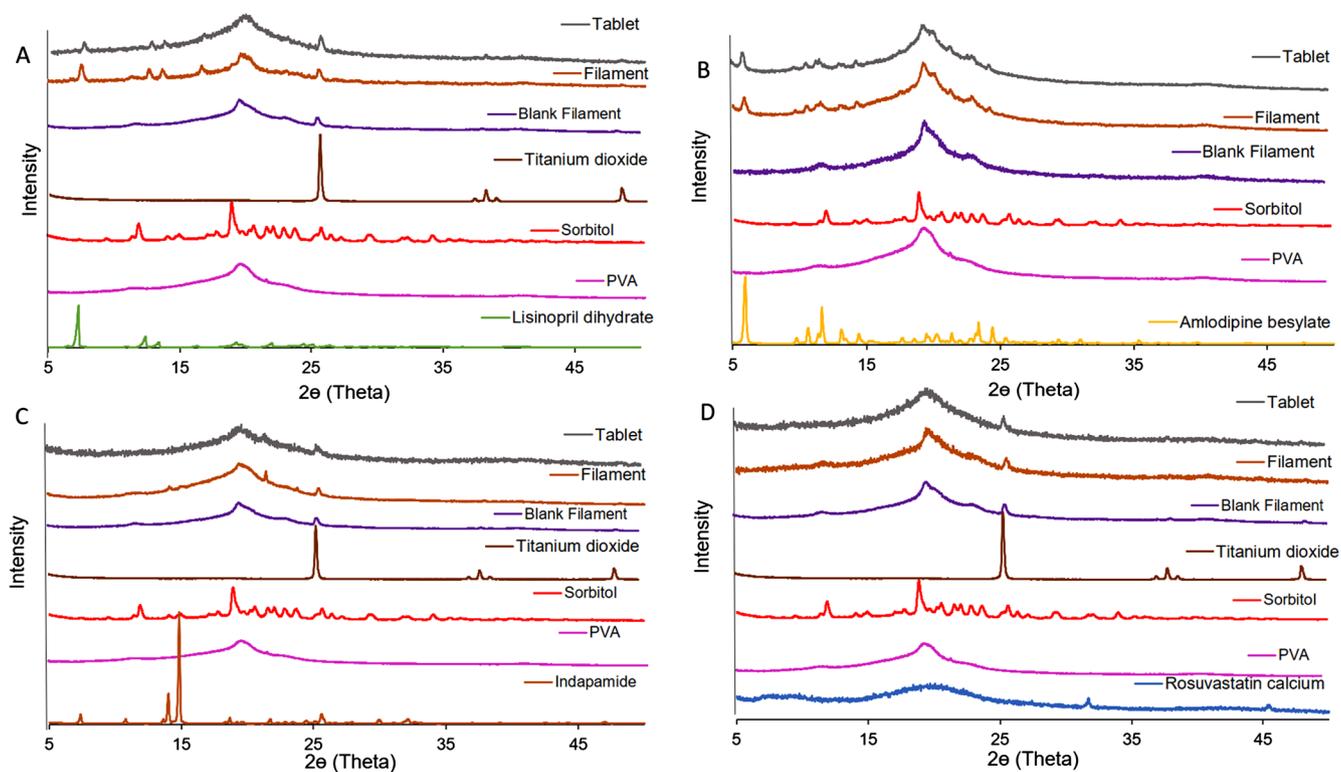

Fig. 6. XRD patterns of raw APIs, PVA, sorbitol, titanium dioxide, blank filament and drug-loaded filaments and 3D printed tablets for (A) lisinopril dihydrate, (B) amlodipine besylate, (C) indapamide and (D) rosuvastatin calcium.

different and were found to be approximately 32.4, 44.7, 17.8 and 22.80 °C for filaments containing lisinopril dihydrate, amlodipine besylate, indapamide and rosuvastatin calcium, respectively (Fig. 5). The higher Tg values in the second heating run are believed to result from the plasticising effect being more due to sorbitol and potentially, the drug on the polymeric chains. It was also noticed that the crystalline domain of PVA was affected by the extrusion and addition of model drug(s), water and sorbitol to the polymeric matrix. The melting point of PVA decreased from 192 to 175 °C in a printable blank filament (after drying for 1 hr). Loading the filaments with drugs decreased the melting of the crystalline PVA component by 2–7 °C (Fig. 5).

DSC thermographs showed the absence of the endothermic peak for the melting of sorbitol (99 °C) or indeed for any of the drugs. The presence of a broad endothermic peak at around 175 °C, thought to be related to the melting of PVA crystalline domains, might have obscured the melting endotherms of the model drugs. Moreover, the evaporation of water from the filament during the DSC analysis may have also obscured any sorbitol melting point. Therefore, XRD was performed in order to confirm the changes in the physical form of sorbitol and drugs within polymeric matrix (Fig. 6). Although PVA is mainly present in an amorphous form, it presents a diffraction peak at (2θ) = 21.5°, which indicates that a small percentage of polymer is in a crystalline form [35]. The data suggests that such a semi-crystalline form remained when other excipients (PVA/sorbitol/titanium dioxide/water) were added. Titanium dioxide retained its crystalline behaviour when it was loaded within the polymeric matrix. This was noted by the presence of the diffraction peaks at 2θ of 25°, 37.9° and 48.1°. These peaks are identical to the previously identified diffraction peaks for titanium dioxide [56]. Similarly, sorbitol exhibited crystallinity when it was used in the preparation of the filaments revealing a characteristic diffraction peak at 2θ of 11.9° [57]

XRD data of filaments and tablets containing lisinopril dihydrate showed diffraction peaks at $2(\theta)$ = 7.5°, 12.5°, 13.6°, and 16.5° which are the distinct diffraction peaks of the crystalline drug (Fig. 6A) [44]. Similarly, filaments and tablets containing amlodipine besylate exhibited XRD patterns with peaks at $2(\theta)$ = 5.8°, 9.7°, 10.6°, 11.4°, 11.7°, 13.2°, 13.7°, and 14.4° consistent with crystallinity [58]. However, the presence of the crystalline form for the other two drugs was not confirmed in all cases (Fig. 6b). Despite the fact that hot melt extruded filaments containing indapamide revealed characteristic diffraction peaks at $2(\theta)$ of 14.1°, 21.4°, and 23.8° [45], XRD patterns of the 3D printed tablets produced from the same filaments did not (Fig. 6c). It is possible that the high noise-to-signal ratio in the tablet scan could have masked the diffraction patterns of indapamide crystals within the noise and the amorphous diffraction pattern of the polymer. On the other hand, the diffraction patterns of both filaments and tablets exhibited no visible matching peaks to rosuvastatin calcium diffraction patterns (Fig. 6d) [59]. This may reflect the amorphous nature of this drug inside the extruded filaments as well as the 3D printed tablets. However, it is worth mentioning that the intensity of the semi-crystalline raw rosuvastatin calcium was very low (around 3 counts). Therefore, it is possible that the diffraction peaks were not visible due to the low intensity and the amorphous nature of the polymer which dominated the diffraction patterns obtained. Notably, in the unimatrix filament and tablet, the diffraction peaks characteristic of the four drugs were absent in XRD data, which might suggest an absence of crystallinity for all drugs. (Supplementary data Fig. S4). However, the absence of characteristic crystalline diffraction peaks could also be due to the relatively low loading percentage of the drugs (5–1.25%) in the filament, compared to the individual drug filaments.

Previous work with 3D printed PVA tablets showed that the drug release was through an erosion-mediated process [17,60,61]. In this research, individual tablets were designed in order to have a large surface area, enhancing the dissolution rate of the drugs. The individual tablets showed a rapid release in gastric medium, with > 80% of drug dissolved in 30 min for lisinopril dihydrate (86.9%), amlodipine
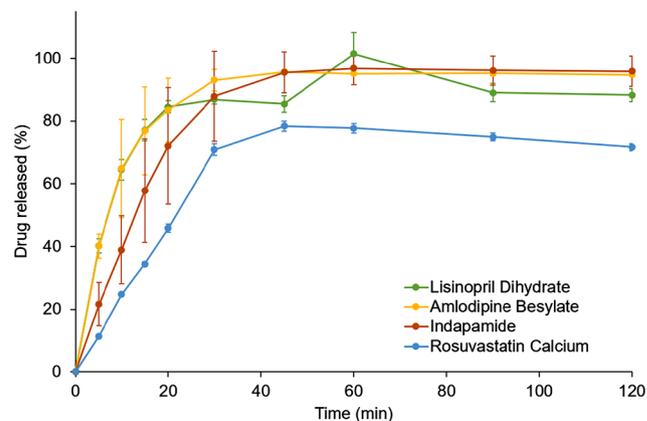

Fig. 7. *In vitro* release of model drugs from individual mono-drug tablets in gastric medium using USP II dissolution test, (pH 1.2), n = 3, mean ± SD.

besylate (93.1%) and indapamide (87.9%) (Fig. 7). Rosuvastatin demonstrated a slower release with 70.9% of the drug dissolved in 30 min, probably due to its poorer solubility in aqueous media [62].

In the unimatrix polypills, drug release was slower in comparison to the individual tablets (Fig. 8a). This may have resulted from the smaller surface area-to-mass ratio of the unimatrix tablet in comparison to individual drug tablets. The slower release highlights the common problem of achieving an immediate drug release from a polymer-rich matrix [63]. It is worth noting that drug release from the unimatrix tablet appeared to be dependent on the solubility of each drug. This resulted in slower rosuvastatin release in comparison with the other model drugs.

On the other hand, when considering of the dissolution profiles obtained from Multilayer I and II polypill formats, the release profile of each drug was dependent on the position of the layer and distinctively different to the release obtained from the unimatrix tablet (Fig. 8b and c). Since the access to water is different for the outer drug layers compared to the inner ones, the tablets showed a biphasic drug release, with initial slow dissolution of some drugs that became faster after a lag time of 15 min. Initially, the drugs in the inner layers only dissolve after diffusion of liquid inwards from the top and lower layers and by erosion from the outermost part of the layer. With time, the top and bottom layers become thinner and effectively shorten the diffusion pathways reaching and from the middle layers to the dissolution medium. The biphasic effect was most clearly observed in Multilayer I, most notably shown in the rosuvastatin release profile, and was most pronounced due to the poor solubility of this particular drug (Fig. 8b). In the Multilayer II format, rosuvastatin and indapamide dissolved faster than Multilayer I (Fig. 8c), a finding that clearly highlights the importance of optimising the order of the drug layers to achieve a desirable drug release from a multilayer tablet design.

Although the relatively modern grade of PVA (Parteck MXP) used in this study was originally designed for boosting the dissolution of poorly soluble drugs [42], the drug release from the matrix block appeared to be hindered by erosion and diffusion mechanisms. The inclusion of a hydrophilic molecule in PVA matrix (i.e. sorbitol) resulted in a significant drop in the Tg of the mixture and likely increased inter-chain spaces within the polymer. The larger spacing may have acted to facilitate water up-take by the polymeric matrix and accelerate the swelling of PVA matrix [64]. After introducing the 3D printed tablets to gastric medium, aqueous penetration was accelerated in line with the above theory. Our results were consistent with the formation of a glassy/rubbery interphace with the dissolution medium, which hindered drug diffusion from the matrix as also identified by others [65]. Therefore, a careful design and sequencing of drug-loaded layers is essential to meet the dissolution criteria of immediate release oral products.
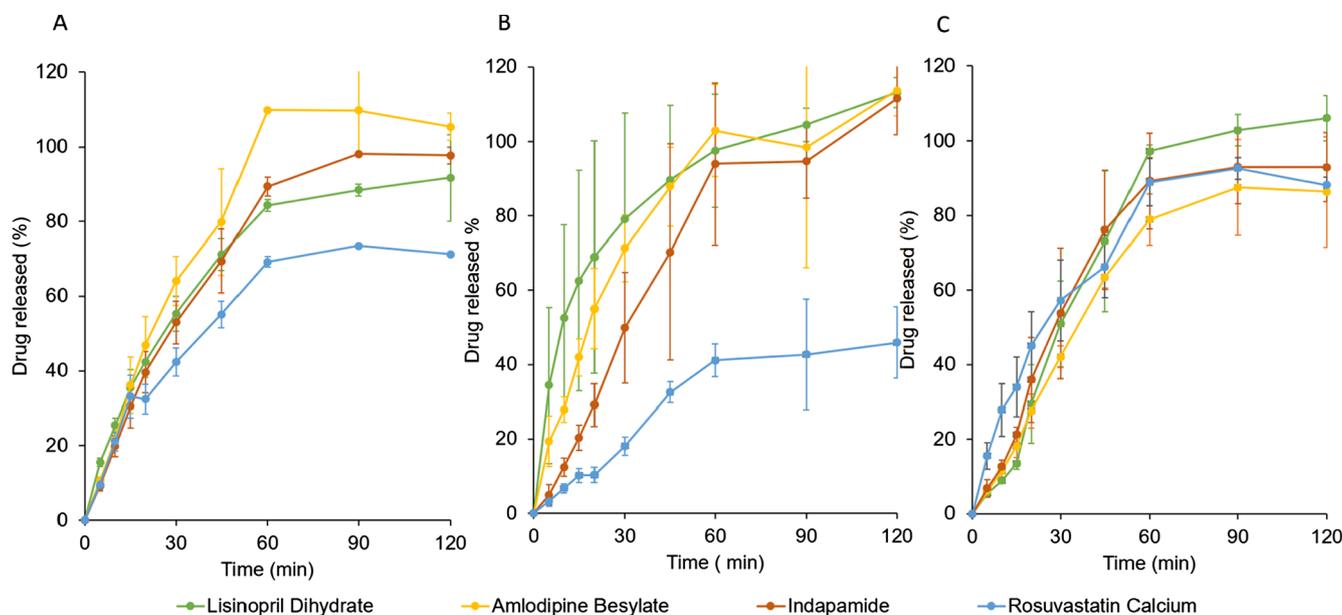
Fig. 8. *In vitro* release of the multiple four drugs from polypill (A): Unimatrix, (B) Multilayer I and (C) Multilayer II tablets in gastric medium using USP II dissolution test, (pH 1.2), n = 3, mean ± SD.

The adaptation of unimatrix tablet approach can be attained using a single filament, which implies significant savings in production steps and costs. However, it is associated with increased risk of stability concerns and precludes the important option of individual dose titration of each drug. On the other hand, the multilayer approach does not only offer higher flexibility in dose titration and a more adaptive solution to meet the expectations of patient-centred therapy, but also allows orchestrating the release of drugs of different physicochemical characteristics.

4. Conclusion

We have explored the consequences of using a temporary plasticiser to permit lower processing temperatures and the significance of polypill architecture on drug release. Given the low cost of FDM 3D printing and the increasing number of reports for its application in the pharmaceutical and medical fields, we expect that our presented solution to be adopted by future FDM 3D printing attempts. In general, drug release from PVA tablets appeared to be dependent on the solubility of each drug. Using a unimatrix approach yielded tablets with slower drug release than individual tablets. On the other hand, by changing the sequence of drug layers in multilayer polypills architecture, the release profile of drug of different physiochemical properties was co-ordinated. Hence, the proposed systems offer the flexibility of incorporation of multiple drugs in a single tablet with optimised release profile of each active component and individualised doses. These findings are essential in developing low-cost modular systems for on demand manufacturing of individualised multidrug units.

Appendix A. Supplementary material

Supplementary data to this article can be found online at https://doi.org/10.1016/j.ejpb.2018.12.009.

References

[1] A.E. Moran, M.H. Forouzanfar, G.A. Roth, G.A. Mensah, M. Ezzati, C.J. Murray, M. Naghavi, Temporal trends in ischemic heart disease mortality in 21 world regions, 1980 to 2010: the global burden of disease 2010 study, Circulation 129 (2014) (1980) 1483–1492.

[2] L. Wei, T. Fahey, T.M. MacDonald, Adherence to statin or aspirin or both in patients with established cardiovascular disease: exploring healthy behaviour vs. drug

effects and 10-year follow-up of outcome, Br. J. Clin. Pharmacol. 66 (2008) 110–116.

[3] P.M. Ho, T.T. Tsai, T.M. Maddox, J.D. Powers, N.M. Carroll, C. Jackevicius, A.S. Go, K.L. Margolis, T.A. DeFor, J.S. Rumsfeld, D.J. Magid, Delays in filling clopidogrel prescription after hospital discharge and adverse outcomes after drug-eluting stent implantation: implications for transitions of care, Circul. Cardiovasc. Qual. Outcomes 3 (2010) 261–266.

[4] L.A. Garcia Rodriguez, L. Cea Soriano, C. Hill, S. Johansson, Increased risk of stroke after discontinuation of acetylsalicylic acid: a UK primary care study, Neurology 76 (2011) 740–746.

[5] C.A. Jackevicius, M. Mamdani, J.V. Tu, Adherence with statin therapy in elderly patients with and without acute coronary syndromes, JAMA 288 (2002) 462–467.

[6] L.K. Newby, N.M. LaPointe, A.Y. Chen, J.M. Kramer, B.G. Hammill, E.R. DeLong, L.H. Muhlbaier, R.M. Califf, Long-term adherence to evidence-based secondary prevention therapies in coronary artery disease, Circulation 113 (2006) 203–212.

[7] A.N. de Cates, M.R. Farr, N. Wright, M.C. Jarvis, K. Rees, S. Ebrahim, M.D. Huffman, Fixed-dose combination therapy for the prevention of cardiovascular disease, Cochrane Database Syst. Rev. (2014).

[8] WHO, Secondary prevention of non-communicable diseases in low- and middle-income countries through community-based and health service, http://apps.who.int/iris/bitstream/10665/42567/1/WHO_MPN_CVD_2002.01.pdf, (20/02/2018); 2002.

[9] N.J. Wald, M.R. Law, A strategy to reduce cardiovascular disease by more than 80%, BMJ 326 (2003) 1419.

[10] J. Tamargo, J.M. Castellano, V. Fuster, The fuster-CNIC-ferrer cardiovascular polypill: a polypill for secondary cardiovascular prevention, Int. J. Cardiol. 201 (Suppl 1) (2015) S15–22.

[11] A. Guglietta, M. Guerrero, Issues to consider in the pharmaceutical development of a cardiovascular polypill, Nat. Clin. Prac. Cardiovasc. Med. 6 (2009) 112–119.

[12] A. Roy, N. Naik, K. Srinath Reddy, Strengths and limitations of using the polypill in cardiovascular prevention, Curr. Cardiol. Rep. 19 (2017) 45.

[13] M.A. Alhnan, T.C. Okwuosa, M. Sadia, K.W. Wan, W. Ahmed, B. Arafat, Emergence of 3D printed dosage forms: opportunities and challenges, Pharm. Res. 33 (2016) 1817–1832.

[14] S.A. Khaled, J.C. Burley, M.R. Alexander, J. Yang, C.J. Roberts, 3D printing of five-in-one dose combination polypill with defined immediate and sustained release profiles, J. Control. Rel.: Offi. J. Control. Rel. Soc. 217 (2015) 308–314.

[15] S.A. Khaled, J.C. Burley, M.R. Alexander, J. Yang, C.J. Roberts, 3D printing of tablets containing multiple drugs with defined release profiles, Int. J. Pharm. 494 (2015) 643–650.

[16] A. Goyanes, A.B. Buanz, A.W. Basit, S. Gaisford, Fused-filament 3D printing (3DP) for fabrication of tablets, Int. J. Pharm. 476 (2014) 88–92.

[17] J. Skowyra, K. Pietrzak, M.A. Alhnan, Fabrication of extended-release patient-tailored prednisolone tablets via fused deposition modelling (FDM) 3D printing, Euro. J. Pharm. Sci.: Offi. J. Euro. Federat. Pharm. Sci. 68 (2015) 11–17.

[18] K. Liang, S. Carmone, D. Brambilla, J.-C. Leroux, 3D printing of a wearable personalized oral delivery device: a first-in-human study, Sci. Adv. 4 (2018).

[19] M. Sadia, A. Sosnicka, B. Arafat, A. Isreb, W. Ahmed, A. Kelarakis, M.A. Alhnan, Adaptation of pharmaceutical excipients to FDM 3D printing for the fabrication of patient-tailored immediate release tablets, Int. J. Pharm. 513 (2016) 659–668.

[20] N.G. Solanki, M. Tahsin, A.V. Shah, A.T.M. Serajuddin, Formulation of 3D printed tablet for rapid drug release by fused deposition modeling: screening polymers for drug release drug-polymer miscibility and printability, J. Pharm. Sci. 107 (2018)

390–401.

[21] W. Kempin, V. Domsta, G. Grathoff, I. Brecht, B. Semmling, S. Tillmann, W. Weitschies, A. Seidlitz, Immediate release 3D-printed tablets produced via fused deposition modeling of a thermo-sensitive drug, Pharm. Res. 35 (2018) 124.

[22] A. Goyanes, F. Fina, A. Martorana, D. Sedough, S. Gaisford, A.W. Basit, Development of modified release 3D printed tablets (printlets) with pharmaceutical excipients using additive manufacturing, Int. J. Pharm. 527 (2017) 21–30.

[23] T.C. Okwuosa, B.C. Pereira, B. Arafat, M. Cieszynska, A. Isreb, M.A. Alhnan, Fabricating a shell-core delayed release tablet using dual FDM 3D printing for patient-centred therapy, Pharm. Res. 34 (2017) 427–437.

[24] A. Goyanes, A.B. Buanz, G.B. Hatton, S. Gaisford, A.W. Basit, 3D printing of modified-release aminosalicylate (4-ASA and 5-ASA) tablets, Eur. J. Pharm. Biopharm. 89 (2015) 157–162.

[25] K. Pietrzak, A. Isreb, M.A. Alhnan, A flexible-dose dispenser for immediate and extended release 3D printed tablets, Eur. J. Pharm. Biopharm. 96 (2015) 380–387.

[26] T. Tagami, K. Fukushige, E. Ogawa, N. Hayashi, T. Ozeki, 3D printing factors important for the fabrication of polyvinylalcohol filament-based tablets, Biol. Pharm. Bull 40 (2017) 357–364.

[27] G. Verstraete, A. Samaro, W. Grymonpré, V. Vanhoorne, B. Van Snick, M.N. Boone, T. Hellemans, L. Van Hoorebeke, J.P. Remon, C. Vervaet, 3D printing of high drug loaded dosage forms using thermoplastic polyurethanes, Int. J. Pharm. 536 (2018) 318–325.

[28] J. Zhang, W. Yang, A.Q. Vo, X. Feng, X. Ye, D.W. Kim, M.A. Repka, Hydroxypropyl methylcellulose-based controlled release dosage by melt extrusion and 3D printing: structure and drug release correlation, Carbohydr. Polym. 177 (2017) 49–57.

[29] A. Goyanes, J. Wang, A. Buanz, R. Martínez-Pacheco, R. Telford, S. Gaisford, A.W. Basit, 3D printing of medicines: engineering novel oral devices with unique design and drug release characteristics, Mol. Pharm. 12 (2015) 4077–4084.

[30] A. Maroni, A. Melocchi, F. Parietti, A. Foppoli, L. Zema, A. Gazzaniga, 3D printed multi-compartment capsular devices for two-pulse oral drug delivery, J. Cont. Rel. 268 (2017) 10–18.

[31] N. Genina, J.P. Boetker, S. Colombo, N. Harmankaya, J. Rantanen, A. Bohr, Anti-tuberculosis drug combination for controlled oral delivery using 3D printed compartmental dosage forms: from drug product design to in vivo testing, J. Control. Rel.: Offi. J. Control. Rel. Soc. 268 (2017) 40–48.

[32] J. Goole, K. Amighi, 3D printing in pharmaceutics: a new tool for designing customized drug delivery systems, Int. J. Pharm. 499 (2016) 376–394.

[33] M. Alhijjaj, P. Belton, S. Qi, An investigation into the use of polymer blends to improve the printability of and regulate drug release from pharmaceutical solid dispersions prepared via fused deposition modeling (FDM) 3D printing, Eur. J. Pharm. Biopharm. 108 (2016) 111–125.

[34] A. Goyanes, M. Kobayashi, R. Martinez-Pacheco, S. Gaisford, A.W. Basit, Fused-filament 3D printing of drug products: microstructure analysis and drug release characteristics of PVA-based caplets, Int. J. Pharm. 514 (2016) 290–295.

[35] Q. Li, H. Wen, D. Jia, X. Guan, H. Pan, Y. Yang, S. Yu, Z. Zhu, R. Xiang, W. Pan, Preparation and investigation of controlled-release glipizide novel oral device with three-dimensional printing, Int. J. Pharm. 525 (2017) 5–11.

[36] D. Smith, Y. Kapoor, A. Hermans, R. Nofsinger, F. Kesisoglou, T.P. Gustafson, A. Procopio, 3D printed capsules for quantitative regional absorption studies in the GI tract, Int. J. Pharm. 550 (2018) 418–428.

[37] T. Tagami, N. Nagata, N. Hayashi, E. Ogawa, K. Fukushige, N. Sakai, T. Ozeki, Defined drug release from 3D-printed composite tablets consisting of drug-loaded polyvinylalcohol and a water-soluble or water-insoluble polymer filler, Int. J. Pharm. 543 (2018) 361–367.

[38] R. Bettini, D. Acerbi, G. Caponetti, R. Musa, N. Magi, P. Colombo, D. Cocconi, P. Santi, P.L. Catellani, P. Ventura, Influence of layer position on in vitro and in vivo release of levodopa methyl ester and carbidopa from three-layer matrix tablets, Eur. J. Pharm. Biopharm. 53 (2002) 227–232.

[39] F. Sonvico, C. Conti, G. Colombo, F. Buttini, P. Colombo, R. Bettini, M. Barchielli, B. Leoni, L. Loprete, A. Rossi, Multi-kinetics and site-specific release of gabapentin and flurbiprofen from oral fixed-dose combination: in vitro release and in vivo food effect, J. Contr. Rel. 262 (2017) 296–304.

[40] NICE, National Institute of Health and Care Excellence: Treatment steps for hypertension, in: https://pathways.nice.org.uk/pathways/hypertension#path=view%3A/pathways/hypertension/treatment-steps-for-hypertension.xml&content=view-index, (01/03/2018); 2018.

[41] P.A. James, S. Oparil, B.L. Carter, W.C. Cushman, C. Dennison-Himmelfarb, J. Handler, D.T. Lackland, M.L. LeFevre, T.D. MacKenzie, O. Ogedegbe, S.C. Smith Jr., L.P. Svetkey, S.J. Taler, R.R. Townsend, J.T. Wright Jr., A.S. Narva, E. Ortiz, Evidence-based guideline for the management of high blood pressure in adults: report from the panel members appointed to the eighth joint national committee (JNC 8), JAMA 311 (2014) (2014) 507–520.

[42] Merck, Parteck® MXP-technical information, in: http://www.merckmillipore.com/GB/en/products/small-molecule-pharmaceuticals/formulation/solid-dosage-form/parteck-excipients/parteck-mxp/Ieyb.qB.lAcAAAFYLEQeWww_,nav, (5/04/2018); 2016.

[43] USP, The United States Pharmacopeial Convention, Amlodipine Besylate Tablets: Revision Bulletin http://www.uspnf.com/sites/default/files/usp_pdf/EN/USPNF/amlodipineBesylateTabletsm3575.pdf, (05/03/2018); 2011.

[44] M. Sorrenti, L. Catenacci, D.L. Cruickshank, M.R. Caira, Lisinopril dihydrate: single-crystal x-ray structure and physicochemical characterization of derived solid forms, J. Pharm. Sci. 102 (2013) 3596–3603.

[45] M. Smrkolj, A. Meden, Crystal structure of indapamide determined from powered diffraction data, Die Pharm. 61 (2006) 999–1004.

[46] P. Sakellariou, A. Hassan, R.C. Rowe, Phase separation and polymer interactions in aqueous poly(vinyl alcohol)/hydroxypropyl methylcellulose blends, Polymer 34 (1993) 1240–1248.

[47] T.C. Okwuosa, D. Stefaniak, B. Arafat, A. Isreb, K.W. Wan, M.A. Alhnan, A lower temperature FDM 3D printing for the manufacture of patient-specific immediate release tablets, Pharm. Res. 33 (2016) 2704–2712.

[48] W. Grymonpré, W. De Jaeghere, E. Peeters, P. Adriaensens, J.P. Remon, C. Vervaet, The impact of hot-melt extrusion on the tableting behaviour of polyvinyl alcohol, Int. J. Pharm. 498 (2016) 254–262.

[49] Merck, Parteck MXP: Technical Informatiol; 2016.

[50] H. Tian, D. Liu, Y. Yao, S. Ma, X. Zhang, A. Xiang, Effect of sorbitol plasticizer on the structure and properties of melt processed polyvinyl alcohol films, J. Food Sci. 82 (2017) 2926–2932.

[51] J. Rault, R. Gref, Z.H. Ping, Q.T. Nguyen, J. Néel, Glass transition temperature regulation effect in a poly(vinyl alcohol)—water system, Polymer 36 (1995) 1655–1661.

[52] H. Levine, L. Slade, Water as a plasticizer: physico-chemical aspects of low-moisture polymeric systems, in: F. Franks (Ed.), Water Science Reviews 3: Water Dynamics, Cambridge University Press, Cambridge, 1988, pp. 79–185.

[53] M.K. Vijay K. T., Handbook of Polymers for Pharmaceutical Technologies: bioactive andcompatible, synthetic/hybrid polymers, Scrivener Publishing LLC; 2016.

[54] H.G. Brittain, Analytical Profiles of Drug Substances and Excipients; 1994.

[55] K.M. Tekendra Pant, Robhash Kusam Subedi, In vitro studies of amlodipine besylate tablet and comparison with foreign brand leader in Nepal, Int. J. Pharm. Sci. Res. 4 (2013).

[56] I. Medina-Ramirez, J.L. Liu, A. Hernandez-Ramirez, C. Romo-Bernal, G. Pedroza-Herrera, J. Jauregui-Rincon, M.A. Gracia-Pinilla, Synthesis, characterization, photocatalytic evaluation, and toxicity studies of TiO_2-Fe_3 + nanocatalyst, J. Mater. Sci. 49 (2014) 5309–5323.

[57] M. Nasr, M. Dawood, Sorbitol based powder precursor of cubosomes as an oral delivery system for improved bioavailability of poorly water soluble drugs, J. Drug Deliv. Sci. Technol. 35 (2016) 106–113.

[58] H.D. Williams, L. Ford, S. Lim, S. Han, J. Baumann, H. Sullivan, D. Vodak, A. Igonin, H. Benameur, C.W. Pouton, P.J. Scammells, C.J.H. Porter, Transformation of bio-pharmaceutical classification system class I and III drugs into ionic liquids and lipophilic salts for enhanced developability using lipid formulations, J. Pharm. Sci. 107 (2018) 203–216.

[59] S. Beg, K. Raza, R. Kumar, R. Chadha, O. Prakash, B. Singh, Improved intestinal lymphatic drug targeting via phospholipid complex-loaded nanolipospheres of rosuvastatin calcium, RSC Adv. 6 (2016).

[60] U. Westedt, M. Wittmar, M. Hellwig, P. Hanefeld, A. Greiner, A.K. Schaper, T. Kissel, Paclitaxel releasing films consisting of poly(vinyl alcohol)-graft-poly(lactide-co-glycolide) and their potential as biodegradable stent coatings, J. Control. Rel.: Offi. J. Control. Rel. Soc. 111 (2006) 235–246.

[61] S. Vaddiraju, Y. Wang, L. Qiang, D.J. Burgess, F. Papadimitrakopoulos, Microsphere erosion in outer hydrogel membranes creating macroscopic porosity to counter biofouling-induced sensor degradation, Anal. Chem. 84 (2012) 8837–8845.

[62] B.V. V.B. Akbari, V.H. Mardiya, A.K. Akbari, G. Vidyasagar, Enhancement of solubility and dissolution rate of rosuvastatin calcium by complexation with β cyclodextrin, Int. J. Pharm. Biol. Arch. 2 (2011) 511–520.

[63] M. Sadia, B. Arafat, W. Ahmed, R.T. Forbes, M.A. Alhnan, Channelled tablets: an innovative approach to accelerating drug release from 3D printed tablets, J. Control. Rel.: Offi. J. Control. Rel. Soc. 269 (2018) 355–363.

[64] A. Hasimi, K.G. Papadokostaki, M. Sanopoulou, Mechanisms of diphylline release from dual-solute loaded poly(vinyl alcohol) matrices, Mater. Sci. Eng. C Mater. Biol. Appl. 34 (2014) 369–376.

[65] J.E. Snaar, R. Bowtell, C.D. Melia, S. Morgan, B. Narasimhan, N.A. Peppas, Self-diffusion and molecular mobility in PVA-based dissolution-controlled systems for drug delivery, Magn. Reson. Imag. 16 (1998) 691–694.